Pressure-Dependent Metallic and Superconducting Phases in a Germanium Artificial Metal

H. B. Cui,[1] D. Graf,[1] J. S. Brooks,[1,*] and H. Kobayashi[2]

[1]*Department of Physics and National High Magnetic Field Laboratory, Florida State University, Tallahassee, Florida 32310, USA*
[2]*Department of Chemistry, College of Humanities and Sciences, Nihon University, Tokyo 156-8550, Japan*
(Received 3 February 2009; published 8 June 2009)

Germanium (Ge) becomes an "artificial metal" and a superconductor ($T_c \sim 5$ K) above the pressure-induced semiconductor-(diamond structure)-to-metal (β-Sn structure) transition at 10 GPa. We report single crystal resistance studies of the pressure-dependent metallic and metastable phases in the range 2.6 to 23 GPa, and show for a controlled pressure release, Ge is a metastable metal below 3 GPa. We find Ge has a superconducting upper critical field of 300 Oe (at 10.7 GPa and 1.8 K), above which a positive magnetoresistance consistent with that of a compensated closed orbit metal is observed.

DOI: 10.1103/PhysRevLett.102.237001 PACS numbers: 74.62.Fj, 61.50.Ks, 74.25.Fy, 81.30.Hd

Artificial metals include nonmetal Group III–VII undoped elements which become metallic, and generally superconducting with transition temperatures (T_c) and critical pressures (P_c) in the approximate ranges $T_c \sim$ 1–30 K and $P_c \sim$ 10–100 GPa, respectively. The elements B [1], Si and Ge [2], P [3], As [4], Sb [5], O [6], S [7], Se [8], Te [9], Br [10], and I [11] are examples. Focusing on Si and Ge, an essential feature is the pressure-induced transformation of the ambient pressure crystal structure to new crystallographic symmetries that (a) are metallic with bands at the Fermi level and (b) create low energy phonon modes that promote electron-phonon interactions leading to superconductivity. Pressure-induced transitions change the crystal symmetry, and nonhydrostatic shearing (symmetry breaking) conditions can both expedite and broaden the transition region. Early on Wittig noted the correspondence between the Grüneisen lattice temperature and the superconducting transition temperature in Si and Ge [2], and Cohen and co-workers have subsequently made a number of detailed electronic structure calculations for Si for both compression [12–15] and decompression (metastable) phases [16]. The results yield the phonon spectrum, the electron-phonon coupling through the Eliashberg formula, the density of states, and realistic predictions of the superconducting transition temperature (via the McMillan relation) vs pressure for different crystal symmetries. Since the high pressure of the nonmetal-to- metal transitions generally require diamond anvil cell methods (with the associated level of difficulty), systematic electrical transport investigations of the metallic and superconducting phases of single crystal samples with temperature, pressure, and magnetic field are very limited.

In the present work, we consider the temperature and magnetic field dependent electrical conductivity of Ge at high pressures for both compression and decompression. The work addresses the following important issues involving artificial metals: (i) the role of hydrostatic conditions and associated methods, (ii) a demonstration that the metastable decompressed BC8 phase is metallic, a result consistent with recent *ab initio* calculations for Si [16], (iii) a description of the superconducting critical field and normal state magnetoresistance, and iv) a motivation for future artificial metal physics in high magnetic fields.

At room temperature Ge has a cubic diamond structure (GeI). At 10 GPa GeI changes to the white tin (β-Sn or GeII) structure [17–25] (see Fig. 1), accompanied by a semiconducting-to-metallic transition [17,26]. Superconductivity was first reported in polycrystalline Ge at 11.5 GPa ($T_c = 5.35$ K) [27], and later the T_c-P phase diagram ($dT_c/dP \sim -0.7$ K/GPa) was resistively determined with single crystals [28]. Interestingly, for an initial pressure above 12 GPa, the GeII structure does not return to the native diamond GeI structure when the pressure is released, but forms metastable structures that are strongly dependent on the pressure release process. A rapid decrease in pressure to ambient pressure from above 11 GPa yields a body centered cubic phase GeIV. This form is not stable, and transforms to the GeI phase in less than a day at room temperature [19,21,24,25]. However, for the slow release of pressure (over several days to low pressure in pressure release steps $\leq$1 GPa), the structure changes to the metastable high density body centered-tetragonal (BC8) phase (GeIII) [17,19,21,22]. The GeIII

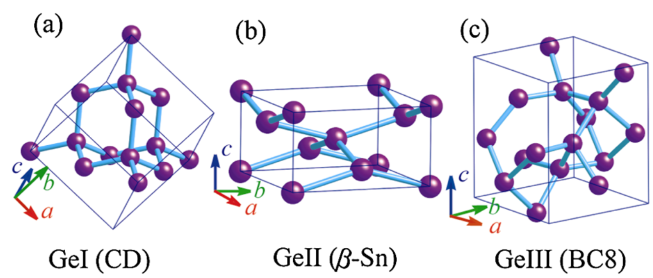

FIG. 1 (color online). Pressure-dependent structural phases of germanium (cell parameters after Qadri *et al.* [24]). (a) GeI: The semiconducting diamond structure for $P < P_c$ ($P_c \sim 10$ GPa). (b) GeII: The metallic and superconducting β-Sn structure for $P > P_c$. (c) GeIII: The metastable, low pressure body centered-tetragonal structure for $P < P_c$ after depressurization from GeII (shown herein to be metallic).

phase is quite stable at room temperature, but reverts to the GeI phase with moderately elevated temperature (over several days at 100 °C). Although the GeIII state was first reported as semiconducting [17], we will show it is actually metallic, in agreement with recent predictions for the BC8-type structure [16].

Single crystal Ge samples (purity 99.999%, Alfa Aesar) were used in all measurements. Two samples, 1 and 2, were cut into rectangular shapes ($0.15 \times 0.05 \times 0.02$ mm^3) and mounted in a similar manner for the diamond anvil cell (see Refs. [29,30]). Sample 2, however, was covered with an epoxy-alumina mixture to reduce the interaction of the pressure medium with the surface. The pressure, determined by ruby fluorescence, was changed at room temperature. The temperature dependence of the resistance for sample 2 is shown in Fig. 2 for different pressures, and the pressure dependence of the resistance at room temperature, 100 K, and 10 K (in the normal state above the superconducting transition) is shown in Fig. 3(a).

The GeI–GeII phase transition occurs sharply [Fig. 3(a)] at 10.1 GPa for sample 2 (with the protective covering), where the sample 2 resistance became simultaneously measurable, fully metallic, and superconducting below 5 K (Fig. 2). For sample 1, in the less hydrostatic environment the resistance (not shown), becomes measurable at 6 GPa, superconductivity is evident at 8.7 GPa ($T_c = 5$ K), but even above 10 GPa, the room temperature resistance is still decreasing significantly with pressure. (For sample 1, the broader range of pressures of the GeI–GeII structural transition is related to differences in the pressure medium induced shear stress [17,23].) Above the critical pressure of the GeI–GeII transition, the resistances of both samples exhibit metallic behavior ($dR/dT > 0$), as shown in Fig. 2 for sample 2, and remains approximately constant below 25 K until the superconducting transition is reached. Below T_c, the resistivity decreases abruptly. Because of the very low resistance in the metallic phase, currents of order 500 μA were used to obtain an acceptable signal to noise level. However, even currents of 5 mA or higher still show

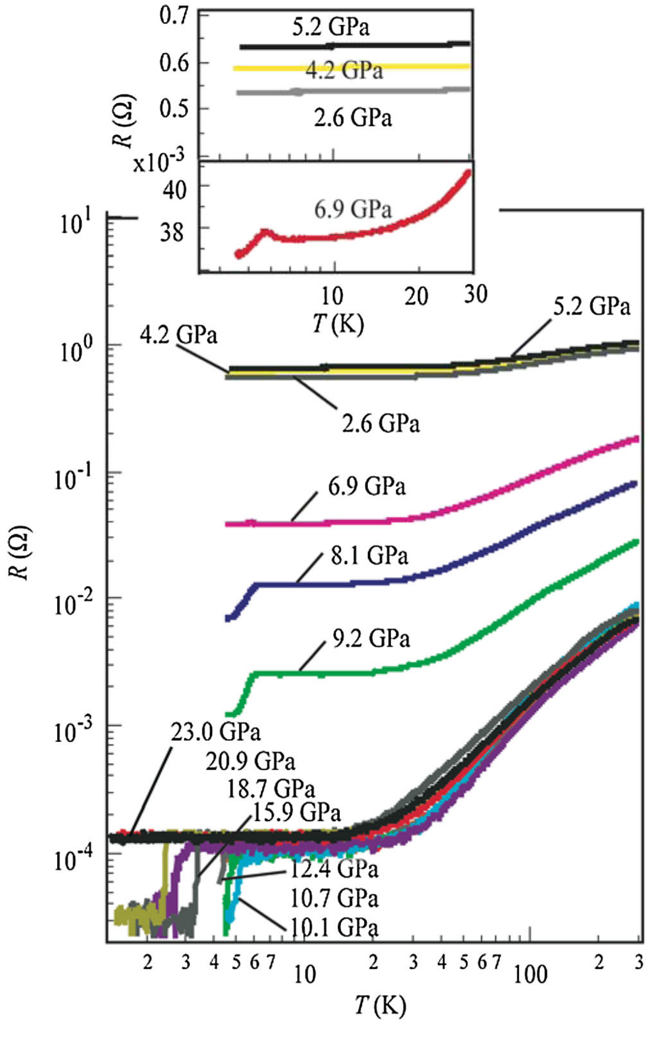

FIG. 2 (color online). The temperature and pressure dependence of the resistance of Ge (sample 2). The sequence of pressures are: 0, (~1.5 GPa/4–5 h up to 8), 9.5, 10.7, 18.7; slow pressure release to 15.0, 14.2, 12.4, 10.7, 10.1, 9.2, 8.1, 6.9, 2.6; slow pressure rise to 4.2, 5.2,10.7, 15.9, 20.9, 23.0; then release to 22.0 (GPa). Inset: Detail of temperature dependent resistance after depressurization at lower pressures.

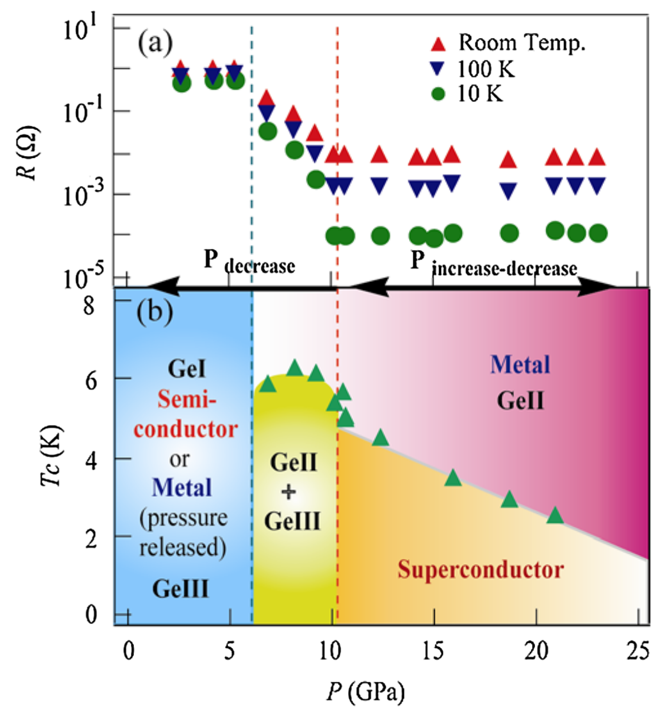

FIG. 3 (color online). Pressure-dependent phases of Ge. (a) Resistance vs pressure at room temperature, 100 K, and 10 K (see Fig. 2 caption for pressure sequence). (b) Temperature pressure-phase diagram. For increasing pressure, at 10.1 GPa the resistance becomes metallic, and superconducting. For pressure release below 10 GPa, superconductivity persists in the mixed GeII + GeIII phase until 6.9 GPa. At lower pressures, only the metallic GeIII phase remains. (The uncertainly in the pressure determined from the ruby fluorescence, ~0.5 GPa, is about the size of the symbols.)

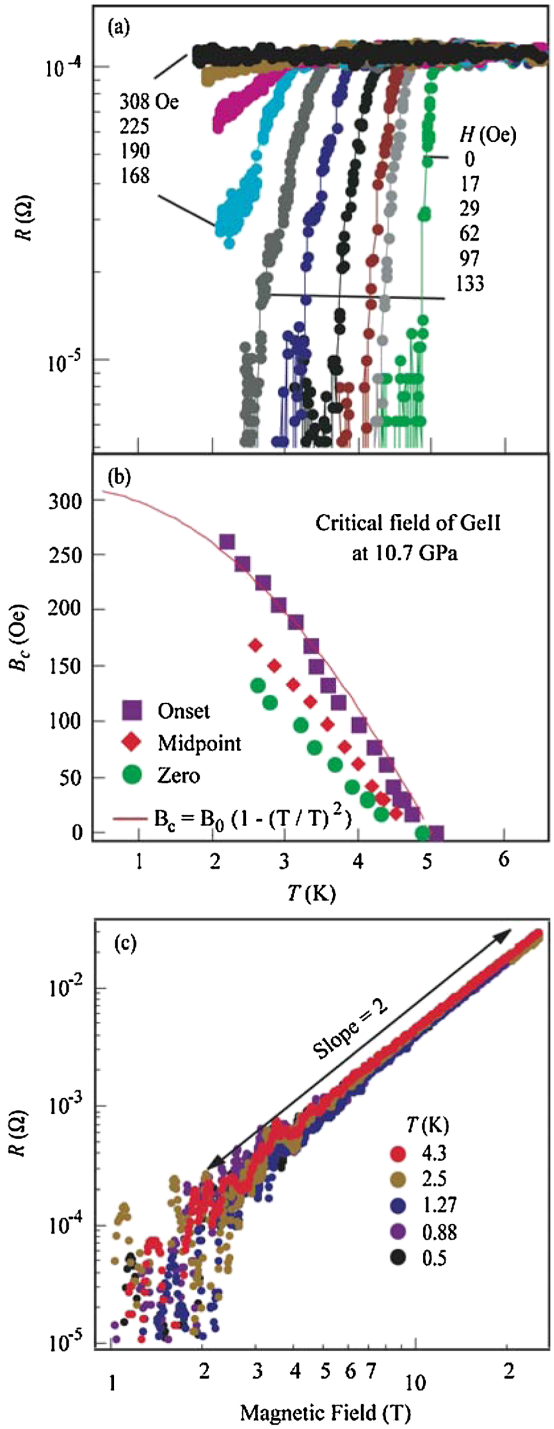

FIG. 4 (color online). The magnetic field dependent resistance of Ge at 10.7 GPa (sample 2). (a) The superconducting transition in resistance vs temperature for different magnetic fields. (b) Superconducting critical field B_c vs temperature based on the magnetoresistive transitions in Fig. 4(a): "Onset" indicates the first drop in the resistance from the normal value; "Midpoint" indicates the point where the resistance is 50% of the normal value; "Zero" indicates the point where the resistance reaches the background noise level. The parameters of the empirical fit to B_c for the Onset curve are $B_0 = 310$ Oe and $T_c = 5$ K. (c) The high field (quadratic) magnetoresistance at various temperatures.

an abrupt resistance drop at the superconducting transition, indicating a bulk superconducting phase.

Sample 2 was slowly depressurized from 15.0 to 2.6 GPa in steps of 1 GPa or less in any one 24 h time interval, and the low pressure GeIII behavior of the temperature dependent resistance after pressure release is shown in Fig. 2. Below the critical pressure of 10 GPa, the resistivity began to rise, but remained metallic, and remnants of the superconducting transition persisted down to 6.9 GPa. Metallic behavior remained to the lowest pressure studied, 2.6 GPa. To the best of our knowledge this is the first report of a low pressure completely metallic phase in Ge (i.e., the BC8 GeIII is metallic). The remnant superconductivity between 9.2 and 6.9 GPa we believe is due to a minority GeII superconducting phase. A summary of the pressure-phase relationships is shown in Fig. 3(b), where we conclude that the structural transition of GeII to GeIII covers a much larger depressurization range than does the abrupt GeI to GeII transition during pressurization. At least in the region between 6.9–9.2 GPa the two structures GeIII and GeII coexist, and the temperature dependence exhibits mixed phase properties. Although beyond the scope of the present work, it is interesting to note that T_c appears to be slightly enhanced in the mixed phase, as observed in both samples.

The superconducting and normal metallic properties of the GeII phase were examined vs temperature and magnetic field for sample 2. The current was parallel to a crystallographic cleavage direction (undetermined) and perpendicular to the field direction. Here the measurements were performed after the pressure was decreased from 18.7 GPa to 10.7 GPa. The superconducting critical magnetic field B_c and temperature T_c were obtained from magnetoresistance measurements as shown in Figs. 4(a) and 4(b). Based on the critical field behavior [see Fig. 4(b)], the superconductivity appears to be type I, and follows relatively closely the empirical quadratic dependence [31] on temperature. The estimated zero temperature critical field is very close to that of β-Sn [32], i.e., $B_c(0) \sim 300$ Oe. (Very few critical fields have been measured in artificial metals: for oxygen [6], $B_c = 2000$ Oe at 0.1 K ($T_c = 0.6$ K, $P_c \sim 100$ GPa), and for sulfur [7] $B_c \sim 5$ T at 25 K ($T_c \sim 10$ to 30 K, $P_c \leq 100$ GPa.) We also measured the magnetoresistance up to 25 T for different temperatures as shown in Fig. 4(c). Between 4.2 and 0.5 K, there is no significant change in the magnetoresistance, which is consistent with the fact that the residual resistivity (of order 5.6×10^{-7} Ω cm) is constant below about 20 K, and therefore Kohler's rule [33] is automatically satisfied in this range of temperature. The magnetoresistance in the normal state is quadratic in field, with no evidence of saturation, consistent with that of a compensated metal with no open orbit contribution. The resistivity ratio $\rho(300\text{ K})/\rho(1.5\text{ K})$ for sample 2 is about 250, which indicates a high purity metal, and is normally a sufficient condition to observe, using magnetization methods, de Haas–van Alphen (dHvA) oscillations due to Fermi surface orbits. An estimate of the cyclotron energy-life time criterion ($\omega_c \tau \geq 1$) for dHvA oscillations based on the low temperature resistivity of sample 2 yields values in the range $0.1 < \omega_c \tau < 1$ for 25 T, indicating that high fields are desirable. However, for resistance measurements as in the present case, the very low resistance generally precludes the observation of quantum oscillations (the Shubnikov–de Haas effect) associated with the Fermi surface. To detect quantum oscillations, dHvA measurements would be necessary as has been done for instance in the case of β-Sn at ambient pressure [34].

In summary, we have performed systematic electrical transport studies on single crystals of Ge to pressures of 23.0 GPa, and the main contributions of this work are as follows. It has been shown that the details of the phase transitions between semiconducting (GeI), metallic-superconducting (GeII), and metastable metallic (GeIII) phases are dependent on the degree of hydrostatic pressure and on the rate at which the pressure is changed. These transitions are reversible with pressure, and the GeI–GeII transition proceeds over a narrower range of pressure than does the GeII–GeIII transition. In the latter case, this has been demonstrated by the observation of remnant superconductivity indicating that a minority GeII phase coexists with the GeIII phase in the mixed phase region. In addition, the low pressure GeIII phase prepared under more hydrostatic and controlled pressure release conditions is metallic over the entire range from room temperature to helium temperatures, in agreement with recent *ab initio* calculations on the corresponding BC8 phase in Si [16]. The superconductivity of the GeII phase is a bulk type I superconductor with a critical field comparable to β-Sn. The temperature and magnetic field dependent resistance studies show that GeII is a high quality metal, consistent with a high conversion rate of GeI to GeII above 10 GPa, and the Fermi surface consists primarily of closed orbits. Here we speculate (until dHvA can be performed under very high pressure conditions) that the Fermi surface of GeII may also resemble that of β-Sn. Our work suggests that Fermiology studies on artificial metals (at high pressures, low temperatures, and in high magnetic fields) is a very promising future area for fundamental metals physics.

We would like to thank S. Tozer for use of the ruby fluorescence system. This work was supported in part by NSF DMR-0602859 and performed at the National High Magnetic Field Laboratory, which is supported by NSF Cooperative Agreement No. DMR-0654118, by the State of Florida, and by the DOE.

*brooks@magnet.fsu.edu

[1] M. I. Eremets, V. V. Struzhkin, and H.-K. Mao *et al.*, Science **293**, 272 (2001).
[2] J. Wittig, Z. Phys. **195**, 215 (1966).
[3] I. Shirotani, U. Mikami, and T. Adachi *et al.*, Phys. Rev. B **50**, 16 274 (1994).
[4] J. Wittig, in *High Pressure Science and Technology*, edited by C. Homan, R. K. MacCrone, and E. Whalley (North-Holland, New York, 1984), p. 17.
[5] J. Witting, J. Phys. Chem. Solids **30**, 1407 (1969).
[6] K. Shimizu, K. Suhara, and M. Ikumo *et al.*, Nature (London) **393**, 767 (1998).
[7] G. N. Stepanov and E. N. Yakovlev, JETP Lett. **32**, 643 (1981).
[8] J. Wittig, Phys. Rev. Lett. **15**, 159 (1965).
[9] B. T. Matthias and J. L. Olsen, Phys. Lett. **13**, 202 (1964).
[10] K. Amaya, K. Shimizu, and M. I. Eremetsz *et al.*, J. Phys. Condens. Matter **10**, 11 179 (1998).
[11] K. Shimizu, T. Yamauchi, and N. Tamitani *et al.*, J. Supercond. **7**, 921 (1994).
[12] K. J. Chang and M. L. Cohen, Phys. Rev. B **30**, 5376 (1984).
[13] K. J. Chang, M. M. Dacorogna, and M. L. Cohen *et al.*, Phys. Rev. Lett. **54**, 2375 (1985).
[14] D. Erskine, P. Y. Yu, and K. J. Chang *et al.*, Phys. Rev. Lett. **57**, 2741 (1986).
[15] J. L. Martins and M. L. Cohen, Phys. Rev. B **37**, 3304 (1988).
[16] B. D. Malone, J. D. Sau, and M. L. Cohen, Phys. Rev. B **78**, 035210 (2008).
[17] F. P. Bundy and J. S. Kasper, Science **139**, 340 (1963).
[18] J. C. Jamieson, Science **139**, 762 (1963).
[19] C. S. Menoni, J. Z. Hu, and I. L. Spain, Phys. Rev. B **34**, 362 (1986).
[20] J. S. Kasper and S. M. Richards, Acta Crystallogr. **17**, 752 (1964).
[21] C. H. Bates, F. Dachille, and R. Roy, Science **147**, 860 (1965).
[22] M. Durandurdu, Phys. Rev. B **71**, 054112 (2005).
[23] M. Baublitz, Jr. and A. L. Ruoff, J. Appl. Phys. **53**, 5669 (1982).
[24] S. B. Qadri, E. F. Skelton, and A. W. Webb, J. Appl. Phys. **54**, 3609 (1983).
[25] R. J. Nelmes, M. I. McMahon, and N. G. Wright *et al.*, Phys. Rev. B **48**, 9883 (1993).
[26] S. Minomura and H. G. Drickamer, J. Phys. Chem. Solids **23**, 451 (1962).
[27] W. Buckel and J. Wittig, Phys. Lett. **17**, 187 (1965).
[28] H. Kawamura and K. Tachikawa, J. Phys. Soc. Jpn. **57**, 3289 (1988).
[29] T. Adachi, H. Tanaka, and H. Kobayashi *et al.*, Rev. Sci. Instrum. **72**, 2358 (2001).
[30] H. Cui, Y. Okano, and B. Zhou *et al.*, J. Am. Chem. Soc. **130**, 3738 (2008).
[31] M. Tinkham, *Introduction to Superconductivity* (McGraw-Hill, New York, 1975).
[32] R. W. Shaw, D. E. Mapother, and D. C. Hopkins, Phys. Rev. **120**, 88 (1960).
[33] J. M. Ziman, *Electrons and Phonons* (Clarendon Press, Oxford, 1960).
[34] J. E. Craven, Phys. Rev. **182**, 693 (1969).